Transesterification Process of Waste Cooking Oil: Catalyst Synthesis, Kinetic Study, and Modeling Sensitivity

Isam Janajreh*[1], Mohammad Almusharekh[2], Chaouki Ghenai[3]
[1,2]Department of Mechanical and Materials Engineering, Masdar Institute of Science and Technology
Abu Dhabi, United Arab Emirates,
[3]Department of Mechanical and Ocean Engineering, Florida Atlantic University
Boca Raton, Florida, USA
*Email: ijanajreh@masdar.ac.ae

Abstract

While finding new energy sources and materials is becoming difficult, finding safer and inexpensive waste disposal is near impossible. Recycling and recovery of material gives a glimpse of hope to lessen the enduring environmental stress. For example in the MENA region it is estimated over 20literes of vegetable oil is consumed per capita and over half of it is rejected into the sewer network. Waste oil due to trapped grease, lard, used cooking oil can be collected and transesterified into a suitable grade of Biodiesel. Test shown (by our group and elsewhere) biodiesel can offset a considerable amount of ICE fossil diesel and particularly in counties where this shortage is saddling citizen. Biodiesel also can be sourced from other non-edible crops including jatropha, rapeseed, algal, and hemp. It is near carbon neutral, lower hydrocarbon emission when used cooking oil is used as its feedstock it is becoming a waste management and waste to energy solution. In this work, collected sample of cooking oil is transesterified using the heterogeneous CaO catalyst that extracted from abundant seashell. It is main advantage is the saving of the exhaustive water amount required to neutralize the homogenous catalyst additional to the economic benefits. Kinetic study is also carried out to estimate the rates constants of the three-step as well as the overall reversible trasesterfication reactions of the triglycerides into FAME, glycerol and their intermediates. Finally, a reactive flow in a modular tubular and continuous reactor is carried out and a 66% conversion is attained in a single flow passage. To achieve better conversion metrics longer reactor or multiple chambers is required. In view of this observation, sensitivity study to the methanol lipid ratio at sweeping temperature values and mass flow rates is also carried out and optimal reactor conditions and configuration is inferred.

Keywords: Transesterification, chemical kinetics, reactive flow, waste oil processing, $CaO/CaCO_3$ catalyst

1. Introduction

Biodiesel is considered as a sustainable alternative to diesel fuel as it can be utilized in current IC Diesel engine without any modification. It is transesterified from the combination of methanol or ethanol and triglycerides/lipid to form mono-alkyl Easter under the presence of catalyst. Trapped grease, waste cooking oil, animal fat can all be used as a substitute for the feedstock. Triglyceride and alcohol are immiscible species and the onset of reaction is mass-transfer limited. The immiscibility is reduced as reaction products are produced and the reaction proceed to be kinetically limited [1-7]. Boer and Bahri [8] investigated the state of mixing from esterified two-phase and mass transfer limited flow into dispersed biphasic mixture in none reactive flow. Mixing or induced turbulence, higher reaction temperature, and the increase in the alcohol amount show an enhancement in the preferable forward reaction. Different types of catalysts can be used to produce biodiesel and are categorized into homogeneous catalysts (sodium/potassium hydroxide, sulfuric acid, etc.), heterogeneous catalysts (cation-exchange resin, hydrotalcites, etc.), and enzymes (Chromobacterium viscosum, Candida rugosa, and Porcine pancreas) [3]. Each has pros and cons, e.g. the drawback of the homogenous is inability to regenerate and the generation of toxic water while enzymatic catalyst is highly expensive. Heterogeneous can also be expensive, difficult to synthesize, sensitive to humidity and soluble in alcohol. Therefore the need for a suitable catalyst for transesterification is still at large. This work consider the locally abundant seashell is an economical catalyst source. Stoichiometric speaking, three moles of alcohol is required to one triglyceride to produced three moles of FAME (Fatty Acid Methyl Ester), however higher alcohol molar ratio are deployed since this ratio fails to guarantee satisfactory conversion. Our

latest results and elsewhere [1,2] showed a sigmoidal reaction progressing for the transesterification. Therefore efficient mixing is the key to improve reaction rate as indicated by Boocock et al. [9]. The onset of triglyceride reaction follow is very slow that followed with a sharp increase towards a final asymptotic platue. It is attributed to the reduction in droplets size, consequent surfactant action of intermediate, and the resulted solvent properties of the product biodiesel as also observed by Boocock [9], Ma et al. [10], and Zhou et al. [11] who described the reaction mixture during this stage as a pseudo single phase emulsion. The final reaction stage is attributed to the two-phase reversion as glycerol concentration is increases, and ineffectiveness of the catalyst which dissolve in the produced polar phase, and the depletion of the glycerides reactants.

2. Materials and Method

Initially different waste cooking oil samples was collected from the campus main cafeteria and in campus restaurant. The used oil is of sunflower branded oil as the most comely used oil in the region. The cafeteria serves two meals one for lunch and a 2nd for diner of different courses that some include deep frying while other is a combination of fast food meals. It serves nearly 700 to 900 meals a day and generate/reject up to 100liters of used cooking oil weekly. The collected samples are cloth filtered (20μm) from any suspended residuals and dried using a continuous stirring at 100ºC over the heating pad in preparation for alcohol mixing. High purity 0.9999 methanol is used for all the experiments.

The heterogeneous catalyst CaO for this study was prepared from the seashell that collected locally. Following washing from any suspended salts and ,dirt it was rinsed and oven dried for several hours at near 100ºC. It was then subjected to calcination in a nitrogen environment oven up to 900 ºC for two hours. The solid material after that became hush and easy to to crush. It was then sieved to 1mm mesh size. The XRD was used and a standard sample of CaO Sigma Aldrich was tested and compared against the synthesized CaO sample. Both showed near identical peaks with some CaCO3 component suggesting a good match between the two catalysts. The moderate 1mm mesh size is used to avoid smaller particle suspension with the yield that hinders the separation processing that may require coagulation, precipitation/sedimentation and/or induced centrifuge.

The kinetic study of this work is carried out in the tubular reactor that seeded with the oven activated/calcinated CaO seashell. An upright cylindrical reactor is used as described in figure 1. Detailed drawings of the chambers and their exact dimensions are found elsewhere of the authors' work [3].

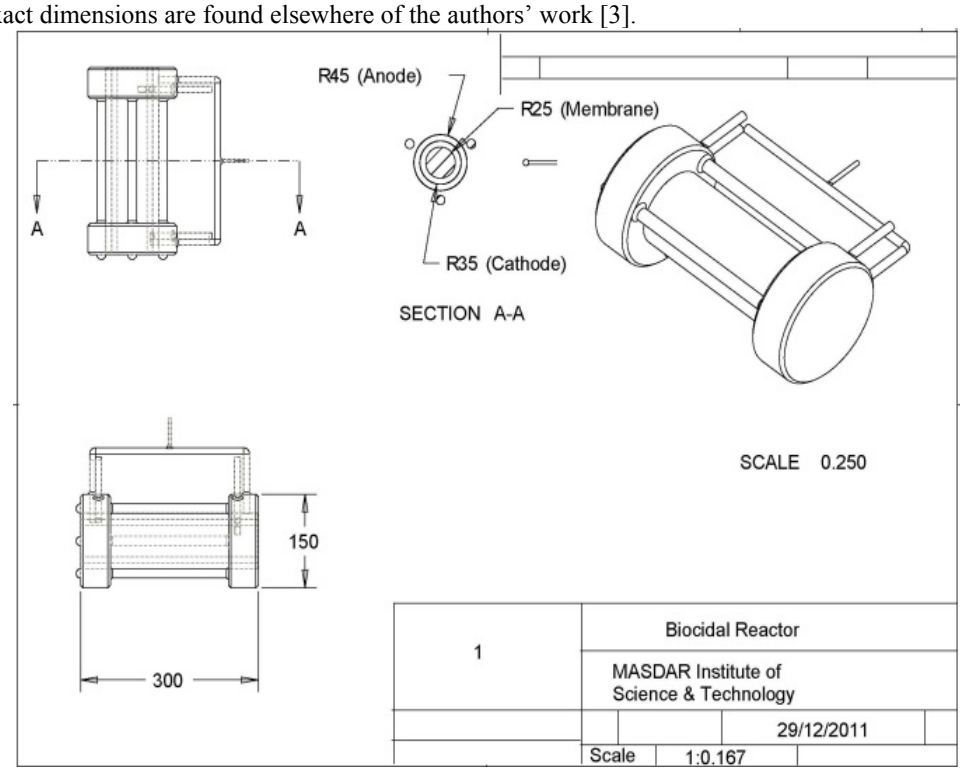

Fig. 1. Geometry specification of the cylinderical transesterification reactor

The analysis of the sample composition as far as Triglyceride, Dioglyceride, Monoglyceride, Easter/FAME and glycerlo is carried out using Thermoscientific DSQ 6000 GC/MS which is equiped with an FID column setup is used to detect the composition of the diffirent smaples obtained at diffirent reaction time step covering two hours reaction time. Samples initially obtained at a few minuts interval to capture the sigmoidal reaction trasition. The procedures of obtaining the breakup of the sample composition of triglyceride, diglyceride, monoglyceride, and alcohol are those carried out by Nourieddine et al.[1] and Janajreh. [3]. Three different columns used in conjunction with the FID method are used in these analysis after running the standard for each as listed in table 1.

Table 1: GC/MS biodiesel column and their specification

Type	Dimensions
TG – 1MS GC	60m X 0.25mm X 0.25µm
TG – 1301MS GC	60m X 0.25mm X 0.25µm
TG – BOND Alumina (KCI)	30m X 0.32mm X 5µm

3. Results of the Kinetic Study

Results of the GC/MS species distribution for each of the TG, DG, MG, FAME and Glycerol for the waste cooking oil at 50^{o}C and 60^{o}C degree temperature are depicted in figure 2.

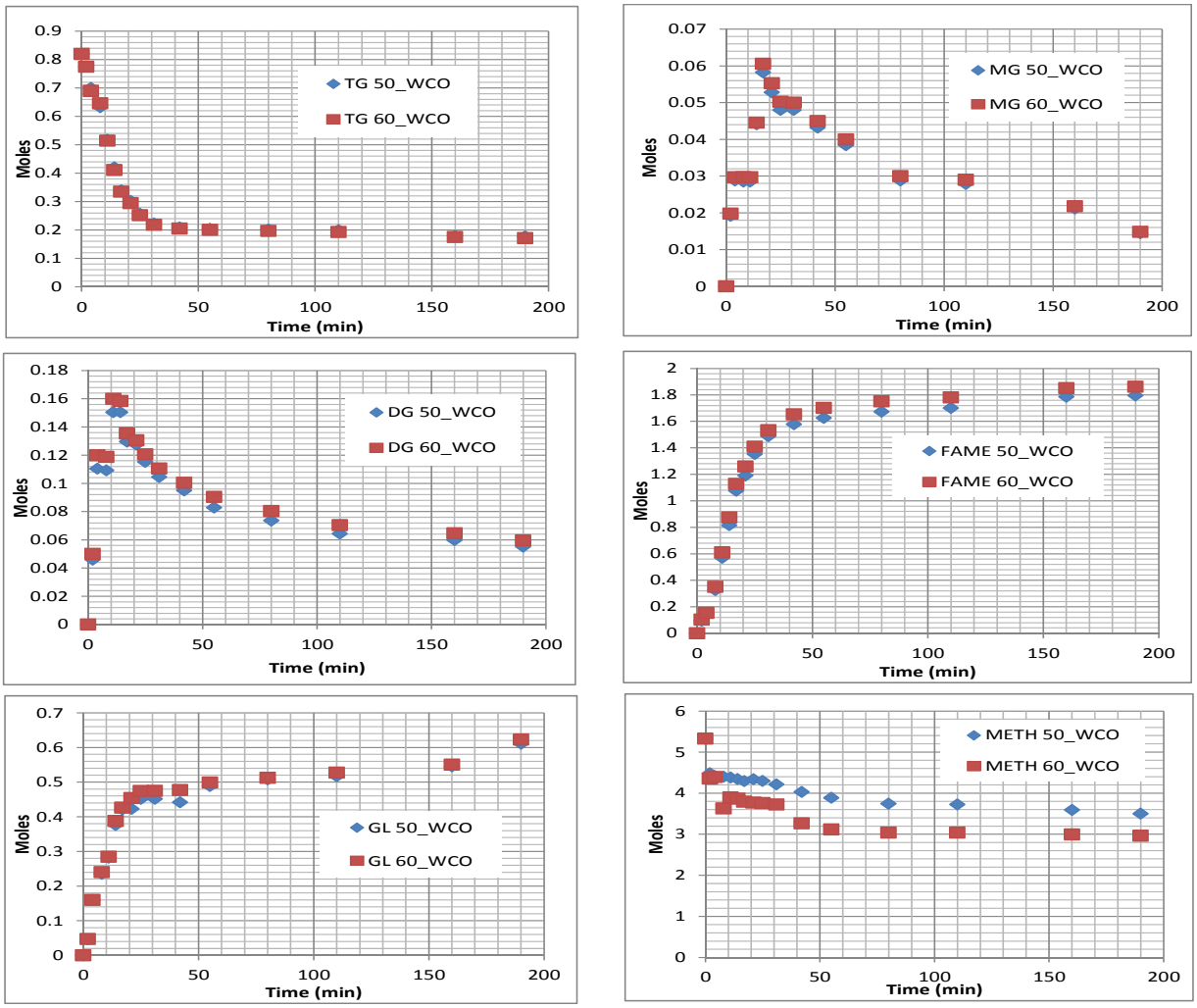

Fig. 2. WCO conversion of each TG, DG, MG, FAME, GL and alcohol at both 50 and 60°C at 6 to1 alcohol waste oil molar ratio.

The transesterification conversion is represented by the three elementary reactions additional to a forth shunt/overall reaction. These are reversible reactions and are governed by the forward and the backward reaction rate constants and are written as:

$$TG + A \underset{k_2}{\overset{k_1}{\rightleftharpoons}} E + DG \quad (1)$$

$$DG + A \underset{k_4}{\overset{k_3}{\rightleftharpoons}} E + MG \quad (2)$$

$$MG + A \underset{k_6}{\overset{k_5}{\rightleftharpoons}} E + GL \quad (3)$$

$$TG + 3A \underset{k_8}{\overset{k_7}{\rightleftharpoons}} 3E + GL \quad (4)$$

Where TG signifies triglycerides, A is alcohol and E, DG, MG, GL are the biodiesel, diglyceride, monoglyceride, and glycerol respectively. Therefore, the above reactions can be mathematically represented by six coupled PDE of the 1st order derivative. This system of PDE is written as:

$$\frac{dTG}{dt} = -K_1[TG][A] + K_2[E][DG] - K_7[TG][A]^3 + K_8[E]^3[GL] \quad (5)$$

$$\frac{dDG}{dt} = -K_3[DG][A] + K_4[E][MG] + K_1[TG][A] - K_2[E][DG] \quad (6)$$

$$\frac{dMG}{dt} = -K_5[MG][A] + K_6[E][GL] + K_3[DG][A] - K_4[E][MG] \quad (7)$$

$$\frac{dE}{dt} = K_1 [TG] [A] - K_2 [E] [DG] + K_3 [DG] [A] - K_4 [E] [MG] + K_5 [MG] [A] - K_6 [E] [GL] + K_7 [TG] [A]^3 - K_8 [E]^3 [GL] \quad (8)$$

$$\frac{dGL}{dt} = K_5 [MG] [A] - K_6 [E] [GL] + K_7 [TG] [A]^3 - K_8 [E]^3 [GL] \quad (9)$$

$$\frac{dA}{dt} = -\frac{dE}{dt} \quad (10)$$

Where [ϕ] signifies the molar concentration of species ϕ , i.e. TG, A, DG, MG, E and GL. The above system is solved for K_1 through K_8 following the measurements of the time evolution of each species. The above system is converted into:

$Ax = b$; and then is solved as: $x = A^{-1}b$ (11)

Where **A** here is the coefficient matrix of the concentrations at each time step and x is the rate constant vector, i.e. k_1 through k_8; and the vector ***b*** is evaluated by the finite time difference of the measurement of the concentration. This system is solved by Matlab at minimum root mean square errors to obtain the vector **x**. The rate constant of each of the eight reactions is expressed as:

$K = Ae^{-E/RT}$ (12)

Where *A (italic)* is the pre-constant, *E (italic)* is the activation energy, R is the universal gas constant and T is the reaction temperature in Kelvin degree.

$$\ln K = \ln A - \frac{E}{R}\frac{1}{T} \quad (13)$$

Therefore, from the slope of the natural log of K vs $\frac{1}{T}$ one can determine the activation energy in J/mole, whereas the intercept of that line is the natural log of the reaction pre-constant. The evaluated GC/MS along with the evaluated rate constant are depicted in figures. Results of the activation energy in comparison to those obtained in the literature are summarized in table 2. It appears that the corresponding reaction rate constants values and the evaluated activation energy are favorably compared.

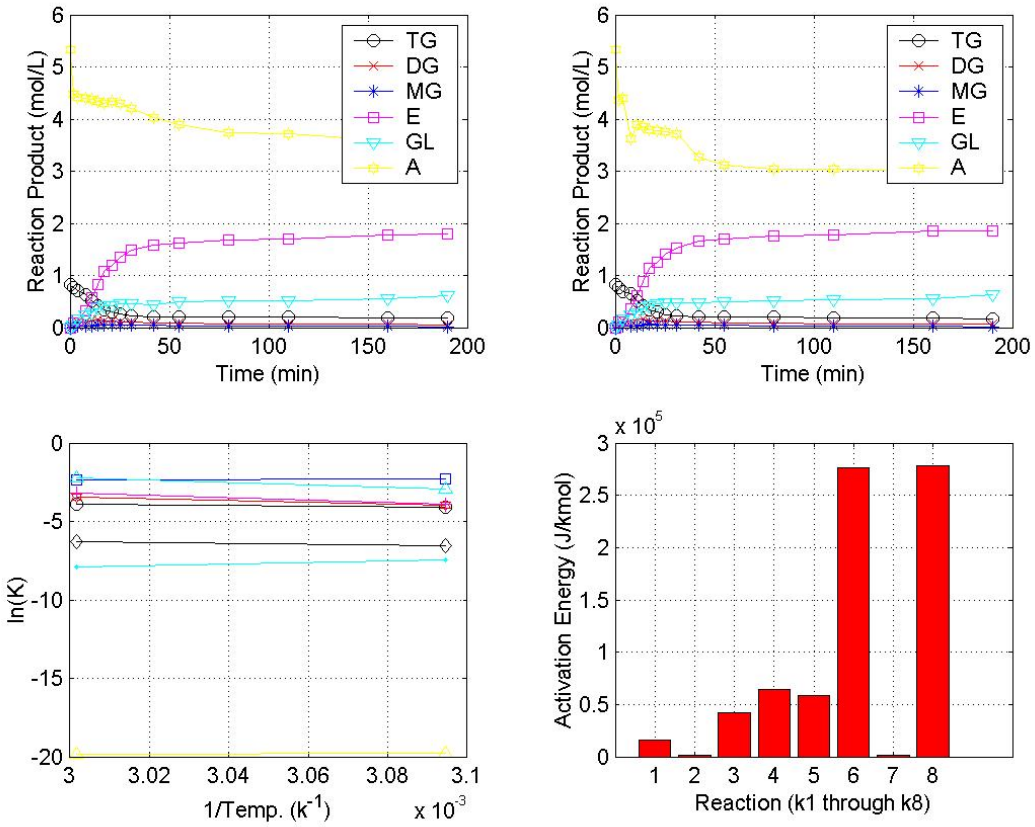

Fig. 3. WCO chemical kinetic results from the conversion at 50 and 60 ºC and corresponding reaction rates values (TG↔DG, DG↔MG,MG↔GL,TG+3A↔3E+GL)

Table 1: Reaction measured rate constant and activation energy compared to those obtained in the literature [9].

Reaction rate constant	**K1**	**K2**	**K3**	**K4**	**K5**	**K6**	**K7**	**K8**
WCO at 50^{O}C (this work)	0.0169	0.0994	0.0194	0.0531	0.0205	0.0015	2.5E-9	0.00056
WCO at 60^{O}C (this work)	0.0202	0.0975	0.0314	0.1106	0.0400	0.0018	2.5E-9	0.00037
Noureddini and Zhu [2]	**0.049**	**0.102**	**0.218**	**1.280**	**0.239**	**0.007**	**7.84E-5**	**1.5E-5**
Activation Energy kJ/kmol	**E1**	**E2**	**E3**	**E4**	**E5**	**E6**	**E7**	**E8**
WCO at 50-60 ^{O}C (this work)	0.1579	0.0172	0.4218	0.6438	0.5865	2.7648	0.01208	0.78100
Noureddini and Zhu [2]	0.0632	0.0477	0.0955	0.0704	0.0308	0.0461	-	-

It should be noted that the adopted kinetic reaction model of these inferred values is a pseudo first-order that combined with shunt-reaction scheme. It is a similar model to that used by the work of Freedman and coworkers [13].

4. Numerical Simulation of Transesterification

The main assumption of the simulation is homogenization of the two reactants at the reactor inlet. This assumption make it possible to proceeds with one phase flow of multiple species. Hence the introduction and development of turbulence by the flow physics including the operating conditions and reactor configuration is a key behind the validity of this assumption.

4.1 Reactor configuration and CFD setup:

An illustration of the transeterfication reactor is depicted figure 1 and the corresponding mesh is shown in figure 4. The tubular reactor consists of two coincided and separated chambers that bring many features including compactness, low pressure drop, ease of temperature control and near isothermal condition additional to the modularity for easy scale up/down. The modularity can be achieved through multiple reactor stack or simply using longer fittings. The reactants are introduced circumferentially and hence it minimizes the pressure drop and increases the residence flow time by following as a swirling trajectory.

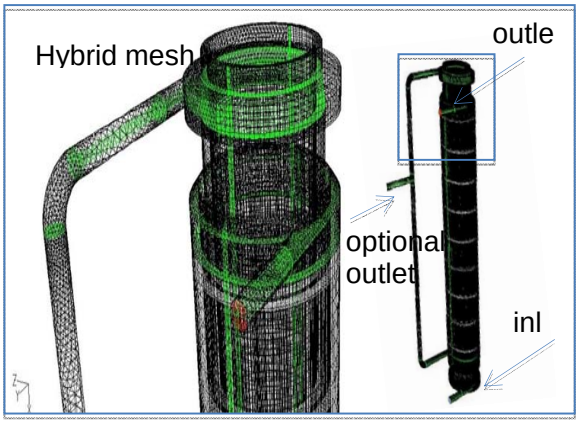

Fig. 4. Reactor discretized mesh

A hybrid hexagonal is generated comprised of 275,00 cells for the two chambers and the connecting tubing as shown in figure 4. The two reactants species are introduce circumferentially the upright reactor at Re 6,000 (based on the bottom inlet diameter of 4mm) into the inner reactor chamber and at the 1:6 triglyceride methanol molar ratio. Atmospheric pressure outlet boundary condition is assigned at the outer tube chamber located at the top. The no slip condition are imposed on all reactors' wall surfaces. Description of the six species are summarized in Table 2. The ideal mixture of weighted mass fraction (m_f) is used to determine the property (ϕ_m) of the mix from single species property (ϕ_i) where is needed.

$$\varphi_m = \sum_{i=1}^{n} m_{f,i}\varphi_i \tag{14}$$

Table 2: Summary of species properties and MW

Species	Chemical formula	Molecular weight	Viscosity (kg/m.s)	Cp (J/kg.^{o}C)	Density Kg/m^3
Methanol	CH_4O	32	3.96E-4	1.470E3	791.8
Waste oil or Triglyceride	$C_{54}H_{105}O_6$	849	1.61E-2	2.2E3	883.3
Diglyceride	$C_{37}H_{72}O_5$	596			880
Monoglyceride	$C_{20}H_{40}O_4$	344			875

Biodiesel	$C_{18}H_{36}O_6$	284	1.12E-3	1.187E3	870
Glycerol	$C_3H_9O_3$	93	1.412E0	0238.6	1261

The operating temperatures values are kept below the boiling point of the methanol at the operating atmospheric pressure. A steady state solution is sought for the flow which enters the reactor by means of an external peristaltic pump at an adjustable flow rate of 50 to 1,000ml/min.

In this work transesterification is attempted at two temperature values (50 ^oC, and 60 ^oC) and at Re beyond the laminar regime that insures the homogeneity of the reactants. Hence, the limited mass transfer initiation stage is avoided and rendering the flow as single phase as indicated also by Boer.

4.2 Governing equations

Modeling reactive flow requires the application of flow continuity, momentum, energy equations, and species transport and turbulence scalars. The onset of transesterification occurs as soon as the reactant components are brought together at the reactor entry. The flow is governed by the Navier-Stokes equations and the associated species transport equation which have the following form:

$$\frac{\partial}{\partial t}(\phi) + \frac{\partial}{\partial x_i}(u_i\phi) = -\frac{\partial}{\partial x_i}\left(\Gamma_\phi \frac{\partial \phi}{\partial x_i}\right) + S_\phi$$

Time rate *advective* *diffusion* *source* (15)

Where u_i is the velocity and S_ϕ is the source term due to destruction or creation of the species by the reaction. ϕ is the dependent variable correspond to the bulk density (ρ) constituting the continuity, the velocity density multiple (ρu_i) constituting the momentum, and the temperature (T) the energy. ϕ can also represent individual specie or turbulent scalars, i.e. Turbulent kinetic energy (k) and the turbulent dissipation rate (ε). The k and ε equations in steady state flow regime are written as:

$$\rho u_i \frac{\partial k}{\partial x_i} = \mu_t \left(\frac{\partial u_j}{\partial x_i} + \frac{\partial u_i}{\partial x_j}\right)\frac{\partial u_j}{\partial x_i} + -\frac{\partial}{\partial x_i}\left(\frac{\mu_t}{\sigma_k}\frac{\partial k}{\partial x_i}\right) - \rho\varepsilon \quad (16)$$

$$\rho u_i \frac{\partial \varepsilon}{\partial x_i} = C_{1\varepsilon}\frac{\mu_t \varepsilon}{k}\left(\frac{\partial u_j}{\partial x_i} + \frac{\partial u_i}{\partial x_j}\right)\frac{\partial u_j}{\partial x_i} + \frac{\partial}{\partial x_i}\left(\frac{\mu_t}{\sigma_\varepsilon}\frac{\partial \varepsilon}{\partial x_i}\right) - C_{2\varepsilon}\frac{\rho\varepsilon^2}{k}$$

The right hand terms are representing the generation, the diffusion, and destruction of the turbulent quantities respectively. In these equations, μ_t is the eddy viscosity which is an order of magnitude higher than the laminar viscosity, it is written as:

$$\mu_t = f_\mu C_\mu \rho k^2 / \varepsilon \quad (17)$$

where f and C are user defined constants and $C_{1\varepsilon}$, $C_{2\varepsilon}$, σ_k and σ_ε are empirical constants. The species m_i transport equation:

$$\frac{\partial}{\partial t}(\rho m_i) + \frac{\partial}{\partial x_i}(\rho u_i m_i) = \frac{\partial}{\partial x_i}\left(\rho D_{i,m} + \mu_t / Sc_t\right)\frac{\partial m_i}{\partial x_i} + R_i \quad (18)$$

Where $D_{i,m}$ is the diffusion coefficient of m_i specie. Sc_t is the turbulent Schmidt number and is defined as the ratio of the eddy viscosity μ_t to the eddy diffusivity $D_{i,m}$. These transport equations incorporate an additional reaction source term R_i that accounts for species reaction and is governed by the stoichiometric reaction below:

$$\sum_{i=1}^{N} \nu'_{i,r} S_i \underset{k_{b,r}}{\overset{k_{f,r}}{\Leftrightarrow}} \sum_{i=1}^{N} \nu''_{i,r} S_i \quad (19)$$

The reaction rate is proportional to the concentration of the reaction products raised to specified power coefficients. That is, the i^{th} species production/destruction due to the reaction r is written as:

$$R_{i,r} = M_{i,r}(\nu''_{i,r} - \nu'_{i,r})\left(k_f \prod_{j=1}^{N} C_{j,r}^{\eta'_{ij}} - k_b \prod_{j=1}^{N} C_{j,r}^{\nu''_{j,r}}\right) \quad (20)$$

where k_f and k_b are the forward and backward reaction constants based on Arrhenius equation (19), C_j is the molar concentration of j^{th} specie raised to stoichiometric coefficients ν and reaction order η, and M_i is the

molecular weight of species *i*.

Initially the CFD analysis is pursued as a none reactive flow to investigate the flow field throughout the tabular reactor, evaluate pressure loss and pressure head/mass flow need. The reactive flow at different flow setting of stoichiometric and over stoichiometric of the methanol lipid (WCO) and temperatures were carried out. These analyses and reaction are developed within the framework of Ansys/Fluent code [15].

The flows simulate an ideal mixture of the two reacting species (methanol and Biodiesel). Figure 1 show the path lines of the mixture colored with the resident times. For the given reactor, the total particle transfer time at relatively 15m/s high velocity is near 0.9 seconds. This value is nearly an order of magnitude higher should the flow introduced along the reactor axis.

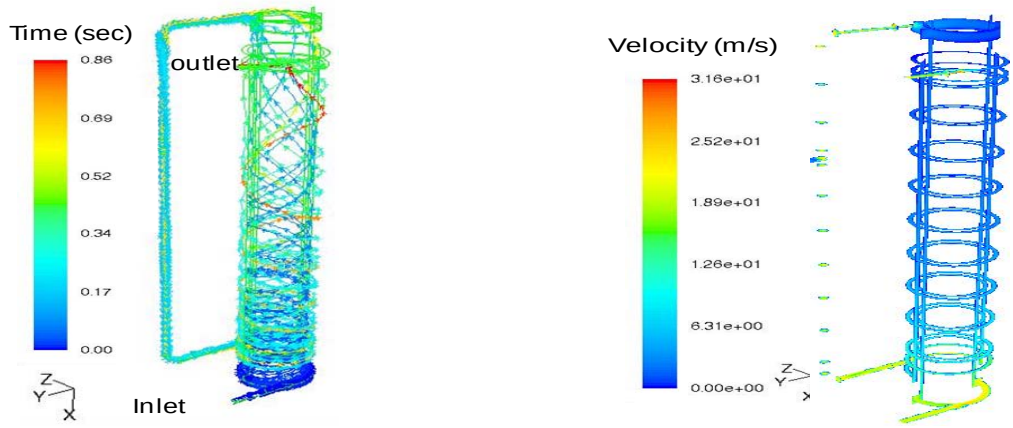

Fig. 5. Flow trajectory colored by the resident time (right) and its velocty (left)

The flow is injected at a relatively high velocity that justified the entering homogenous mixture. The mixture is also entrained in a swirl trajectory that enhances the reactivity and to enjoy a longer residence time. The none reactive flow trajectory colored by the residence time and its velocity contours are depicted in figure 5. Stoichiometry reactive flow is simulated corresponding to three moles of methanol to one mole of WCO (mass ratio of 1:8.745). The model results at the baseline condition of 1 to 3 of waste oil to methanol ratio are presented below in figure 6 and species distribution at the entrance and the exit of the reactor are summarized in table 3.

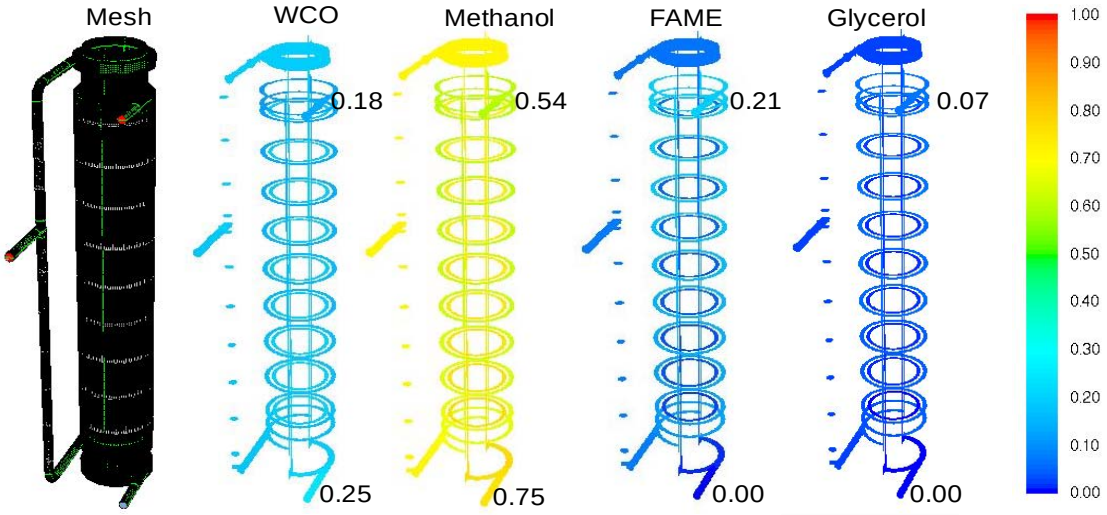

Fig. 6. Molar fraction of species across the reactor (Global scale)

Table 3: Species molar fraction at idealistic conditions

Port & ratio/Species	$C_{54}H_{106}O_6$	CH_4O	$C_{18}H_{36}O_2$	$C_3H_9O_2$	Conversion

	(WCO)		(FAME)		
inlet	0.25	0.75	0	0	28%
outlet	0.18*	0.54	0.21	0.07	

*Conversion=(0.25-0.18)/0.25

At these conditions a low conversion of 28% is achieved which is attributed to the shorter residence time, a low kinetics of the reacting species, as well as lower availability of methanol.

4.3 Sensitivity study:

Modularity of the reactor allow one to carryout sensitivity studies for the different configuration additional to variation of the flow conditions. This includes the effect of the molar ratio, inlet velocity and temperature as well as the reactor size. Results for the influence of the increase in the methanol triglyceride ratio and increase in the inlet flow velocity are shown in figure 7. As the molar ration is increased the rates of the forward reactions dominate the reversible reactions and more lipid conversion takes place. The velocity trend, however is the opposite as higher velocity enable more throughput, it however reduces the residence time and consequently lower conversion occurs.

.

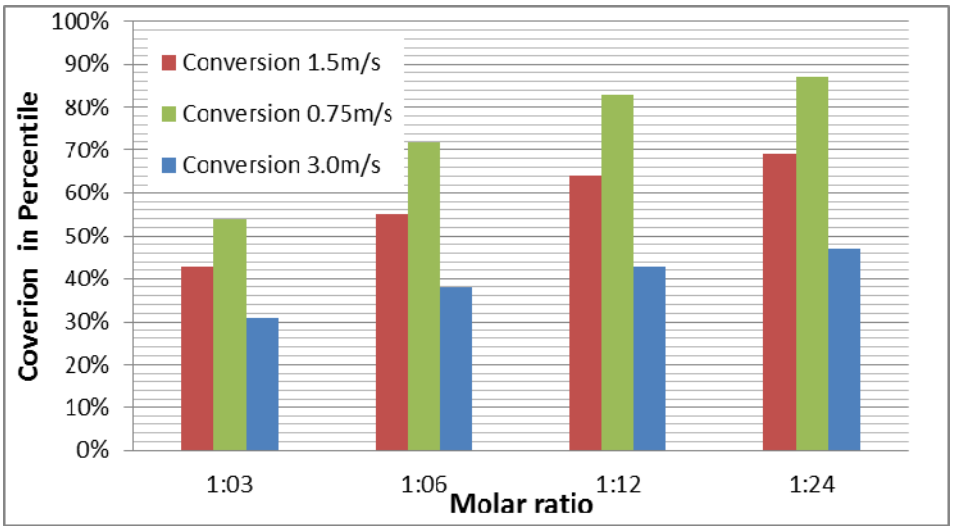

Fig. 7. Influence of molar ratio and velocity

Results of the effect of the inlet reactant temperature are depicted in figure 8. As the reaction is neither exothermic nor endothermic, the temperature effect does not reflect a unified trend and is also less pronounced. It is again may appear counter intuitive as the increase of the temperature resulted in slightly lower conversion. It is however due to the considered revisable reaction which also feeds both ways on the temperature according to their activation energy. In general irreversible reaction rate increase with the increase of the temperature, however reversible reaction has an optimal temperature value for the conversion and the desired yield. Another aspect is the extrapolation of the temperature value beyond the initial tested range. This is typically an overstretch for the validity of the trend beyond what have been tested as in the case for 45^{o}C. Apparently the conversion follow the closely tested temperature trend of 50 ^{o}C. It also should be noted that viscosity is assumed independent of the temperature as that may hinder the reactivity but is not accounted for within the simulation.

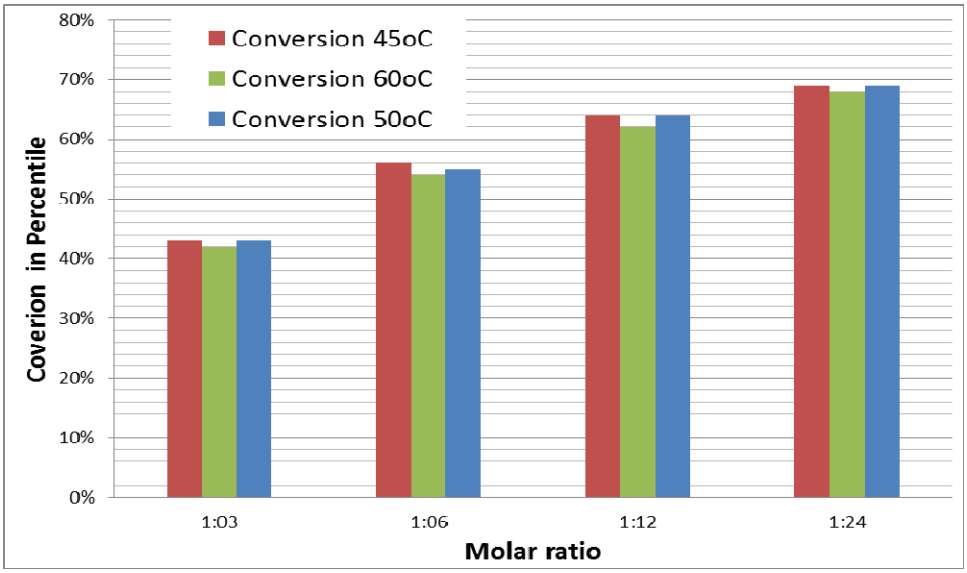

Fig. 8. Influence of the temperature on the conversion

Results of the influence of the reactor size is depicted in figure 9. It clearly shows the pronounced effect of the reactor length which dominates the increase in the diameter or width. This is due to the swirling momentum that is maintained for the longer reactor whereas is faded for wider diameter reactor.

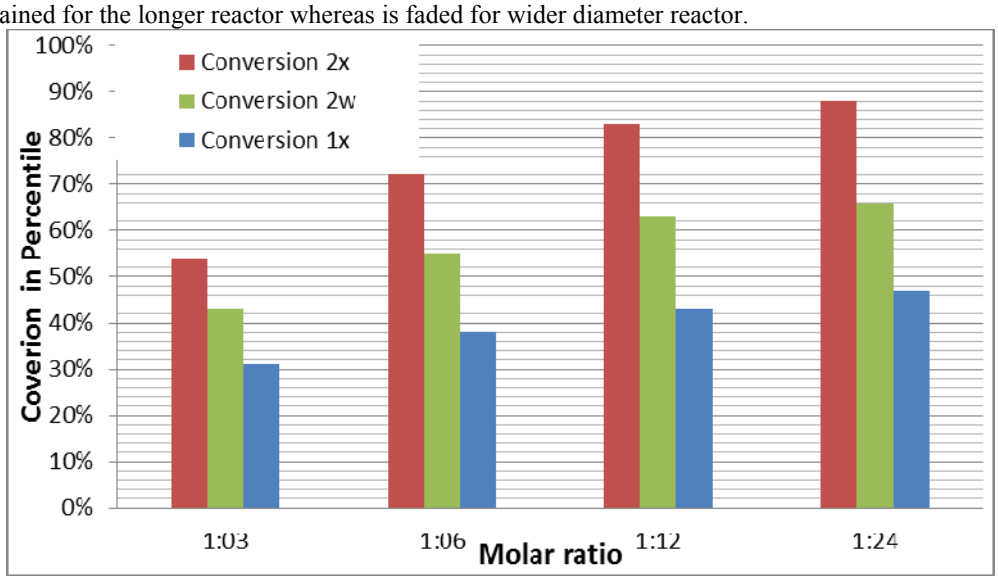

Fig. 9. Influence of the reactor length on the conversion

5. Conclusion

In this work several experiments for the transeterfication of waste cooking oil was carried out using the the synthesized heterogeneous CaO catalyst from the locally abundant seashell. Chemical kinematic study was also carried out and the distribution of the molar composition of the five species including, triglyceride, di-glyceride, mono-glyceride, biodiesel and glycerol was measured using GC/MS equipped with appropriate FAME columns and following FID methodology. The reate of reaction constants as well as their corresponding activation energies for 8 elementary trasnesterification reaction were evaluated. Their rates appears to be lower than those results of Noureddine who used the NaOH as the commoly used homeogenous catalyst. The evaluated rate constants and their activation energy are implemented in high fidelity numerical simulation that produced a good reaction yield trend. The developed model then was subjected to different

sensitivity studies including the molar rate, the inlet velocity, the size of the reactor additional to the inlet temperature. These results have brought more insight to the conversion, i.e. conversion rate, reaction rate, and species distribution. In particular, it shows the conversion is in the favor of the excess amount methanol as well as lower inlet velocity value. The latter is attributed to the longer reaction time. Temperature influence seems counter intuitive due to the inclusion of the revisable reaction however the influence is also is less significant than other parameters including the size. The influence of reactor length is significant as it also attributed to the increase of the reaction time. It is however more dominate than the increase in the reactor diameter/width.

References

[1] H. Noureddini and D. Zhu, "Kinetics of Transesterification of Soybean Oil," Journal of the American Oil Chemists society, vol. 74, no. 11, pp. 1457-1463, 1997.

[2] Stamenkovic O.S., Lazic M.L., Todorovic Z.B., Veljkovic V.B., Skala D.U., Kinetics of sunflower oil methanolysis at low temperatures.Bioresource Technology 99, 1131-1140. (2008)

[3] Janajreh, I. and Al Shrah, M. (2013). "Numerical Simulation of Multiple Step Transesterification of Waste Oil in Tubular Reactor." J. Infrastruct. Syst., 10.1061/(ASCE)IS.1943-555X.0000183 (Aug. 3, 2013)

[4] Ala'a Alsoudy, Mette Thomsen , Isam Janajreh, "Influence of Process Parameters in Transesterification of Vegetable and Waste Oils-A review, International Journal of Research & Reviews in Applied Sciences . 2012, Vol. 10 Issue 1, pg64-77

[5] M. Kee Lam, K. T. Lee and A. R. Mohamed, "Homogeneous, heterogeneous and enzymatic catalysis for transesterification of high free fatty acid oil (waste cooking oil) to biodiesel: A review," *Biotechnology Advances,* no. 28, pp. 500-518, 2010.

[6] R. Abd Rabu, I. Janajreh, D. Honnery, "Transesterification of Waste Cooking Oil: Process Optimization and Conversion Metrics", Energy Conversion and Management, 65 (2013) 764-769

[7] Stamenkovic O.S., Lazic M.L., Todorovic Z.B., Veljkovic V.B., Skala D.U., The effect of agitation intensity on alkali-catalyzed methanolysis of sunflower oil. Bioresource Technology 98, 2688-2699. (2007) .

[8] Karne De Boer and Parisa A. Bahri, Investigation of Liquid-Liquid Two Phase Flow in Biodiesel Production, Seventh International Conference on CFD in the Minerals and Process Industries CSIRO, Melbourne, Australia 9-11 December 2009

[9] Boocok D. GB, Konar S. K, Moa V., Lee C., Buligan S., "Fast formation of high-purity methyl esters from vegetable oils", J. Am. Oil Chem. Soc. 75, 1167-1172, 1998.

[10] Ma F., Clements D., Hanna M. " The effect of mixing on transesterification of beef tallow", Bioresource Technology 69, 289-293, 1999

[11] Zhou W., Boocock G. B, "Phase behavior of the base catalyzed transesterification of soybean oil. J. Am. Oil Chem. Soc. 83, 1041-1045, 2006.

[12] Mohamed Almusharekh, "Transesterification: Continuous Process Development, Kinetic Determination and Reactive Flow Modeling", Masdar Institute thesis data base, Mechanical Engineeirng, May 2014

[13] Reedman, B., R.O.. Butterfield, and E.H. Pryde, Transestrification Kinetics of Soybean Oil, J. Am. Oil Chem, Soc. 63:1375-1380, 1986

[14] Laidler, K., The development of the Arrhenius equation. Journal of Chemical Education, 1984. 61(6): p. 494.

[15] FLUENT, A. 6.3. Theory Manual. 2005. Fluent Inc. Central Source Park, 10 Cavendish Court, Lebanon, NH 03766, USA.